

Liquid-gas phase behaviour of an argon-like fluid modelled by the hard-core two-Yukawa potential

D. Pini

*Istituto Nazionale di Fisica della Materia and Dipartimento di Fisica,
Università di Milano, Via Celoria 16, 20133 Milano, Italy*

G. Stell

*Department of Chemistry, State University of New York at Stony Brook,
Stony Brook, NY 11794-3400, U.S.A.*

N.B. Wilding

*Department of Mathematical Sciences, University of Liverpool,
Peach Street, Liverpool L69 7ZL, U.K.*

Abstract

We study a model for an argon-like fluid parameterised in terms of a hard-core repulsion and a two-Yukawa potential. The liquid-gas phase behaviour of the model is obtained from the thermodynamically self-consistent Ornstein-Zernike approximation (SCOZA) of Høye and Stell, the solution of which lends itself particularly well to a pair potential of this form. The predictions for the critical point and the coexistence curve are compared to new high resolution simulation data and to other liquid-state theories, including the hierarchical reference theory (HRT) of Parola and Reatto. Both SCOZA and HRT deliver results that are considerably more accurate than standard integral-equation approaches. Among the versions of SCOZA considered, the one yielding the best agreement with simulation successfully predicts the critical point parameters to within 1%.

I. INTRODUCTION

Much attention has been paid in recent years to the hard core Yukawa (HCY) potential as a model for the pair interactions of fluids [1]. Interest in the potential is motivated on the one hand by its relevance to solvent averaged interactions in polyelectrolytic and colloidal particles and, on the other hand, by its analytical tractability in the context of liquid state theories such as the Mean Spherical Approximation (MSA) and the Self Consistent Ornstein-Zernike Approximation (SCOZA). Recent studies of the HCY fluid can be found in [2,3] and references therein.

For simple fluids interacting via dispersion forces, however, the bare HCY potential fails to provide a realistic representation of the interactions, which are much better modelled by the Lennard-Jones (LJ) potential. Unfortunately owing to its mathematical structure, the latter is less amenable to direct study by the MSA and SCOZA than is the HCY potential. Nevertheless, it has long been appreciated that a LJ-like simple-fluid potential can be replaced by a potential with a hard core plus a linear combination of *two* Yukawa tails [4–8] with no appreciable loss of agreement between the experimental and model equations of state. Such a potential permits the theoretical study of simple fluids whilst retaining the convenient mathematical properties of the HCY potential.

Several different representations of a LJ-like fluid in terms of a hard-core plus two Yukawa fluid (HC2YF) have been proposed in the literature [4–8]. The one we use here is very similar to that recently given by Kalyuzhnyi and Cummings [9]:

$$v(r) = \begin{cases} \infty & r \leq \sigma, \\ \frac{A_1\epsilon}{r} \exp[-z_1(r - \sigma)] - \frac{A_2\epsilon}{r} \exp[-z_2(r - \sigma)] & r > \sigma. \end{cases} \quad (1.1)$$

Here σ and ϵ set the length and energy scales of the model and coincide with the zero and the well depth of the LJ potential respectively. The parameters $A_1 = 1.6438\sigma$, $z_1 = 14.7\sigma^{-1}$, $A_2 = 2.03\sigma$ and $z_2 = 2.69\sigma^{-1}$ are chosen to fit the LJ potential and match the second virial coefficient to that of the LJ fluid. Eq. (1.1) differs slightly from the original parameterisation by Kalyuzhnyi and Cummings inasmuch as these authors determined the hard-sphere diameter σ_{HS} as a function of temperature via the Barker-Henderson procedure [10] in order to represent the soft-core repulsive interaction which results from the Weeks-Chandler-Henderson separation of the LJ potential [11]. We instead hold the hard-core diameter fixed by setting $\sigma_{\text{HS}} = \sigma$ for conceptual simplicity and clarity in making comparison with our simulation results. A comparison of Eq. (1.1) with the LJ potential is shown in Fig. 1. Kalyuzhnyi and Cummings [9] have used the MSA, Percus-Yevick approximation and reference hypernetted chain theories to obtain the liquid-gas phase behaviour of the HC2YF specified by their parameterisation. Their results showed good agreement with existing literature data for the LJ fluid.

In the present work, we extend the work of Kalyuzhnyi and Cummings [9] by determining the liquid-gas phase behaviour of the HC2YF using the SCOZA of Høye and Stell. Unlike those considered in ref. [9], this theory is neither mean-field nor mean-spherical like and on the basis of a similar study already performed for the HCY fluid, it can be expected to give a superior account of fluid properties in the near-critical regime. We compare the predictions

of the SCOZA for the the critical point and the coexistence curve to those obtained by other approaches, including the renormalization-group based hierarchical reference theory (HRT) of Parola and Reatto [12], and to new high resolution simulation results for the HC2YF. We find that one version of the SCOZA considered provides a remarkably accurate critical point and coexistence curve. The critical density and temperature predicted by the theory agree with the simulation results to within 1%.

II. THEORY

The SCOZA deals with two-body potentials which, like that of Eq. (1.1), consist of a singular hard-sphere repulsion with diameter σ and a longer-ranged tail $w(r)$. As is customary in integral-equation theories, this approach is based upon the Ornstein-Zernike (OZ) equation linking the two-body radial distribution function $g(r)$ to the direct correlation function $c(r)$. A closed theory is obtained by supplementing the OZ equation with an approximate relation involving $g(r)$ and $c(r)$. In its simplest form, the SCOZA amounts to setting:

$$\begin{cases} g(r) = 0 & r < 1, \\ c(r) = K(\rho, \beta)w(r) & r > 1, \end{cases} \quad (2.1)$$

where ρ is the number density of the system, $\beta = 1/(k_B T)$ is the inverse temperature, and the hard-sphere diameter has been set equal to one. This closure resembles that adopted in the MSA, except that the amplitude K of the direct correlation function outside the repulsive core is regarded as an unknown state-dependent quantity, to be determined in such a way that consistency between the compressibility and the energy route to thermodynamics is enforced. This constraint amounts to requiring that the reduced compressibility χ_{red} and the excess internal energy per unit volume u satisfy the condition:

$$\frac{\partial}{\partial \beta} \left(\frac{1}{\chi_{\text{red}}} \right) = \rho \frac{\partial^2 u}{\partial \rho^2}, \quad (2.2)$$

where it is understood that χ_{red} is obtained by the compressibility sum rule as the structure factor $S(k)$ evaluated at $k = 0$, while u is obtained by the energy equation as the spatial integral of the tail interaction $w(r)$ weighted by the radial distribution function $g(r)$. If the closure (2.1) is used for the correlations, the consistency condition (2.2) yields a closed partial differential equation (PDE) for the function $K(\rho, \beta)$. In the present case, implementing this scheme is made simpler by taking advantage of the analytical results obtained for the OZ equation with the closure (2.1) when the tail potential $w(r)$ has a two-Yukawa form like that of Eq. (1.1). These enable one to obtain χ_{red} as a function of ρ and u . The function $\chi_{\text{red}}(\rho, u)$ can then be used in Eq. (2.2) by taking u instead of K as the unknown quantity. The algebraic manipulations are similar (although not identical) to those we performed in Ref. [3], and are based on the results obtained in Ref. [13]. We start by introducing the quantity:

$$f = (1 - \xi) \sqrt{\frac{1}{\chi_{\text{red}}}}, \quad (2.3)$$

where $\xi = \pi\rho/6$ is the packing fraction. This can be written as:

$$f = -\frac{(z_1^2 - z_2^2) + 4\sqrt{q}(\gamma_2 - \gamma_1)}{4[(z_1/z_2)\gamma_2 - (z_2/z_1)\gamma_1]} - \frac{z_1^2 - z_2^2}{z_1 z_2} \frac{\gamma_1 \gamma_2 (\gamma_2 - \gamma_1)}{[(z_1/z_2)\gamma_2 - (z_2/z_1)\gamma_1]^2}, \quad (2.4)$$

where $q = (1 + 2\xi)^2/(1 - \xi)^2$, and γ_1, γ_2 are state-dependent functions. By using Eqs. (2.3) and (2.4), Eq. (2.2) becomes:

$$\frac{2f}{(1 - \xi)^2} \left[\left(\frac{\partial f}{\partial \gamma_1} \right)_{\rho, \gamma_2} \left(\frac{\partial \gamma_1}{\partial u} \right)_\rho + \left(\frac{\partial f}{\partial \gamma_2} \right)_{\rho, \gamma_1} \left(\frac{\partial \gamma_2}{\partial u} \right)_\rho \right] \left(\frac{\partial u}{\partial \beta} \right)_\rho = \rho \left(\frac{\partial^2 u}{\partial \rho^2} \right)_\beta, \quad (2.5)$$

where the partial derivatives of f with respect to γ_1, γ_2 are straightforwardly obtained from Eq. (2.4). In order to obtain a closed PDE for u , one then needs to express γ_1, γ_2 as a function of ρ and u . To this end, we recall the definitions of γ_1, γ_2 [13]:

$$\gamma_i = 2 - \sqrt{q} - \frac{4 + 2z_i - z_i^2}{2(2 + z_i)} \frac{\tau_i I_i - 1}{\sigma_i I_i - 1} \quad (i = 1, 2), \quad (2.6)$$

where the quantities σ_i, τ_i are known and depend only on the inverse range z_i , and I_i is given by:

$$I_i = 4\pi\rho \int_1^{+\infty} dr r \exp[-z_i(r - 1)] g(r) \quad (i = 1, 2). \quad (2.7)$$

For the two-Yukawa tail potential of Eq. (1.1), the integrals I_1, I_2 are straightforwardly related to the internal energy per unit volume u :

$$u = \frac{1}{2} \rho \epsilon (A_1 I_1 - A_2 I_2). \quad (2.8)$$

If Eq. (2.6) is used to express I_i as a function of γ_i and the result is substituted into Eq. (2.8), one obtains an expression for u as a function of ρ, γ_1, γ_2 . This can be inverted algebraically to obtain γ_2 as a function of ρ, γ_1 , and u . One is then left with the task of expressing γ_1 in terms of ρ and u . If we set:

$$x = \sqrt{q} - \frac{z_1^2}{4\gamma_1}, \quad (2.9)$$

$$y = \sqrt{q} - \frac{z_2^2}{4\gamma_2}, \quad (2.10)$$

we find by applying the results of Ref. [13] that the following equation hold:

$$\begin{aligned} & A_2 z_2^4 \sigma_1^2 (2 + z_1)^2 \left[4(2 - \sqrt{q} - \alpha_1)(\sqrt{q} - x) - z_1^2 \right]^2 \left\{ 4(z_2^2 - 4y^2)(y - x)^2 \right. \\ & \quad \left. - (z_1^2 - z_2^2) \left[z_1^2 - z_2^2 + 4(y^2 - x^2) \right] \right\} \\ & - A_1 z_1^4 \sigma_2^2 (2 + z_2)^2 \left[4(2 - \sqrt{q} - \alpha_2)(\sqrt{q} - y) - z_2^2 \right]^2 \left\{ 4(z_1^2 - 4x^2)(y - x)^2 \right. \\ & \quad \left. - (z_1^2 - z_2^2) \left[z_1^2 - z_2^2 + 4(y^2 - x^2) \right] \right\} = 0, \end{aligned} \quad (2.11)$$

where α_i , $i = 1, 2$, are known functions of the inverse-range parameters z_i . Note that this equation does not contain the unknown amplitude $K(\rho, \beta)$. By writing x and y as functions of γ_1 , γ_2 via Eqs. (2.9), (2.10), and subsequently γ_2 as a function of ρ , γ_1 , u , we finally obtain an equation for γ_1 as a function of ρ and u . If we indicate the l.h.s. of Eq. (2.11) by $F(x, y, \rho)$, the equation for γ_1 has the form:

$$F\{x(\gamma_1), y[\gamma_2(\rho, \gamma_1, u)], \rho\} = 0. \quad (2.12)$$

Eq. (2.5) then becomes:

$$B(\rho, u) \left(\frac{\partial u}{\partial \beta} \right)_\rho = C(\rho, u) \left(\frac{\partial^2 u}{\partial \rho^2} \right)_\beta, \quad (2.13)$$

where $B(\rho, u)$ and $C(\rho, u)$ are given by:

$$B(\rho, u) = \frac{2f}{(1-\xi)^2} \frac{\partial \gamma_2}{\partial u} \left[\frac{\partial f}{\partial \gamma_2} \frac{\partial F}{\partial x} \frac{\partial x}{\partial \gamma_1} - \frac{\partial f}{\partial \gamma_1} \frac{\partial F}{\partial y} \frac{\partial y}{\partial \gamma_2} \right], \quad (2.14)$$

$$C(\rho, u) = \rho \left[\frac{\partial F}{\partial y} \frac{\partial y}{\partial \gamma_2} \frac{\partial \gamma_2}{\partial \gamma_1} + \frac{\partial F}{\partial x} \frac{\partial x}{\partial \gamma_1} \right], \quad (2.15)$$

where all the partial derivatives are performed at constant density ρ .

We note that in Eq. (2.1) there is no hard-sphere contribution to the direct correlation function outside the repulsive core. As a consequence, the treatment of thermodynamics and correlations of the hard-sphere gas that come out of Eq. (2.1) in the high-temperature limit coincide with that of the Percus-Yevick (PY) integral equation. An improved description of the hard-sphere thermodynamics at the level of the well known Carnahan-Starling (CS) equation of state is desirable in this context, as the slight inaccuracy in the PY treatment of the hard-sphere gas affects not only the high-density behavior of the system in study, but also the location of its critical point and of the coexistence curve. A non-vanishing contribution to $c(r)$ for $r > 1$ due to hard-core part of the interaction could be taken into account by replacing the expression for $c(r)$ of Eq. (2.1) with

$$c(r) = c_{\text{HS}}(r) + K(\rho, \beta)w(r) \quad r > 1, \quad (2.16)$$

where the hard-sphere direct correlation function $c_{\text{HS}}(r)$ can be determined, for instance, by the Waisman parameterisation [14]. This is what has been done in Ref. [3] for the HCY fluid. However, in the present case of a two-Yukawa tail potential, this would require one to deal with a direct correlation function of three-Yukawa form for $r > 1$. Although such an extension of our treatment appears to be feasible [7], in order to minimize the complexity of the computation, we have not pursued it here. Instead, we assumed for $c_{\text{HS}}(r)$ outside the core a Yukawa form whose range coincides with that of the repulsive contribution to the tail potential, and whose density-dependent amplitude H is set so as to give CS thermodynamics in the high-temperature limit. This procedure does not aim at the most accurate description of the hard-core contribution to the correlations possible in the context of the SCOZA. But it has the advantage of taking into account the hard-sphere thermodynamics beyond the PY level without going beyond the two-Yukawa form of $c(r)$. An analogous procedure involving only a single Yukawa term was already implemented for the HCY fluid [15], where it was

found to give results very similar to those of the more reliable closure (2.16) both for the thermodynamics and the phase diagram. According to this prescription, for $r > 1$, $c(r)$ has the form:

$$c(r) = \frac{(H + KA_1)}{r} \exp[-z_1(r - 1)] - \frac{KA_2}{r} \exp[-z_2(r - 1)] \quad r > 1, \quad (2.17)$$

while for $r < 1$ the core condition $g(r) = 0$ holds as before. Here K is the unknown, state-dependent amplitude of Eq. (2.1), which vanishes in the high-temperature limit, while H is a known function of the density. As the inverse range of the hard-sphere contribution to $c(r)$ is locked to z_1 , the treatment of the hard-sphere gas that comes out of Eq. (2.17) clearly lacks the virial-compressibility consistency of the Waisman parameterisation. However, this does not affect the consistency between internal energy and compressibility route upon which SCOZA hinges. The manipulations that lead to the PDE (2.13) remain unchanged, the only difference being that Eq. (2.11) will contain an extra term related to H , which will affect the partial derivatives $\partial F/\partial x$, $\partial F/\partial y$ that appear in Eqs. (2.14), (2.15).

The PDE (2.13) has been integrated numerically. The initial condition at $\beta = 0$ and the boundary conditions at the ends of the density interval are the same as in Ref. [3] and will not be detailed here. Once u has been obtained by solving Eq. (2.13), integration of u with respect to β yields the Helmholtz free energy and hence all the other thermodynamic quantities.

III. SIMULATION PROCEDURE

The principal aspects of the simulation and finite-size scaling techniques employed in this work have previously been detailed elsewhere in the context of a similar study of the Lennard-Jones fluid. Accordingly we restrict ourself to a brief summary of the methodology and refer the reader to reference [16] for a fuller account.

Grand canonical Monte-Carlo (MC) simulations were performed for the HC2YF model of Eq. (1.1). The algorithm used had a Metropolis form [17] and comprised only particle transfer (insertion and deletion) steps, leaving particle moves to be performed implicitly as a result of repeated transfers. The potential was cut at a radius $r_c = 3.0\sigma$, and a standard correction term was applied to the internal energy to compensate for the truncation [17]. To simplify identification of particle interactions the periodic simulation space of volume L^3 was partitioned into m^3 cubic cells, each of side the cutoff r_c . This strategy ensures that interactions emanating from particles in a given cell extend at most to particles in the 26 neighbouring cells.

System sizes having $m = 3, 4, 5, 6, 7$ and 8 were studied, corresponding (at coexistence) to average particle numbers of approximately 230, 540, 1050, 1750, 2900 and 4500 respectively. For the $m = 3, 4, 5$ and 6 system sizes, equilibration periods of 10^5 Monte Carlo transfer attempts per cell (MCS) were utilised, while for the $m = 7$ and $m = 8$ system sizes up to 2×10^6 MCS were employed. Sampling frequencies ranged from 20 MCS for the $m = 3$ system to 250 MCS for the $m = 8$ system. The total length of the production runs was also dependent upon the system size. For the $m = 3$ system size, 1×10^7 MCS were employed, while for the $m = 8$ system, runs of up to 1×10^8 MCS were necessary.

In the course of the simulations, the observables recorded were the particle number density $\rho = N/V$ and the energy density $u = E/V$. The joint distribution $p_L(\rho, u)$ was accumulated in the form of a histogram. In accordance with convention [17], we express all thermodynamic quantities in reduced units: $\rho^* = \rho\sigma^3$, $u^* = u\sigma^3/\epsilon$, $T^* = k_B T/\epsilon$.

Efficient exploration of the phase space was facilitated through use of the histogram reweighting technique [18]. This method allows histogram accumulated at one set of model parameters to be reweighted to provide estimates appropriate to another set of not-too-distant model parameters. Use of the method permits large areas of phase space to be mapped using only a few simulations performed at strategic state points. To facilitate study of the subcritical coexistence region, the multicanonical preweighting technique [19] was employed. This method employs a biased sampling technique to overcome the free energy barrier separating the coexisting phases and thus allow both to be sampled in a single simulation run. When combined with histogram reweighting in the manner described in ref. [16], multicanonical preweighting permits an extremely efficient accumulation of coexistence curve data.

The task of estimating the critical point parameters of the model was performed using finite-size scaling techniques [16]. In brief, the strategy is to match the measured “ordering operator distribution” to an independently known universal critical point form appropriate to the Ising universality class. The ordering operator itself is defined as $\mathcal{M} \propto (\rho^* + su^*)$, where s is a non-universal “field mixing” parameter, which is finite in the absence of particle-hole symmetry, and which is chosen to ensure that $p(\mathcal{M})$ is symmetric in \mathcal{M} [20]. For sufficiently large L , the matching should occur at the critical point parameters. For small L , however, the apparent critical temperature obtained by this matching procedure is subject to systematic errors associated with corrections to finite-size scaling. To deal with this, we extrapolate to the thermodynamic limit using the known scaling properties of the corrections, which are expected to diminish (for sufficiently large system sizes) like $L^{-\theta/\nu}$ [16], where θ is the correction to scaling exponent and ν is the correlation length exponent. The extrapolation has been performed using a least squares fit to the data for the four largest system sizes. The results of the extrapolation are shown in Fig. 2, from which we estimate $T_c^* = 1.295(10)$. The associated estimate for the critical density is $\rho_c^* = 0.310(1)$ and for the reduced chemical potential is $\mu_c^* = -3.588(30)$.

In addition to the phase coexistence data, we have also measured the form of the radial distribution function $g(r)$ for a number of state points, corresponding to reduced temperatures $T^* = 2, 1.5, 1$, and reduced densities $\rho^* = 0.4, 0.6, 0.8$. In the following Section, the simulation results for the coexistence curve, critical point properties and radial distribution function of the HC2YF are compared with the theoretical predictions.

IV. RESULTS AND DISCUSSION

The SCOZA coexistence curve has been determined by equating the pressure P and the chemical potential μ on the low- and high-density branch of the subcritical isotherms. As we specified above, these quantities were obtained via the energy route by integrating u with respect to β . The advantage of doing so is that one does not have to circumvent the forbidden region bounded by the spinodal curve, i.e. the locus of diverging compressibility, in order to obtain P and μ on the high-density branch. On the other hand, because of the

compressibility–internal energy consistency of the theory, this is fully equivalent to using a mixed path combining integration of the inverse compressibility $1/\chi_{\text{red}}$ with respect to ρ and integration of u with respect to β , as is often done in calculations based on integral equations [2]. The coexistence curve in the density–temperature and in the temperature–chemical potential plane is shown in Figs. 3 and 4 respectively. Reduced units have been used throughout. The SCOZA results obtained both by the closure (2.1) and by the modified version (2.17) are compared with the MC data obtained in this work. We have also plotted the coexistence curve predicted by HRT and by the energy route of the lowest-order gamma-ordered approximation (LOGA) [21], also known as optimized random-phase approximation (ORPA) [22], together with the spinodal curve given by LOGA/ORPA compressibility route. It appears that the SCOZA yields the most accurate determination of the coexistence curve among the theories considered here, provided Eq. (2.17) is used in order to describe hard-sphere thermodynamics at the CS level. The predictions for the critical point are compared in Tab. I. The error on the SCOZA critical density and temperature is below 1%. Actually, the critical temperature predicted by SCOZA with closure (2.1) and PY hard-sphere thermodynamics is even closer to the MC result, but this is most likely to be accidental since, as stated in Sec. II, on the basis of our previous calculations on the HCY potential [3] we expect that a treatment of the HC2YF based on closure (2.16) and a $c(r)$ of three-Yukawa form will in fact deliver results almost identical to those found here by Eq. (2.17). We note that, like the HRT or the energy-route LOGA/ORPA, the SCOZA gives a coexistence curve that goes right up to the critical point. This feature is not shared by other integral-equation approaches, such as the MHNC or the HMSA theories [2]. Both the SCOZA below the critical temperature and the HRT yield non-classical critical exponents; for the exponent β_{coex} which describes the curvature of the coexistence curve the SCOZA gives $\beta_{\text{coex}} = 7/20 = 0.35$ [23], while according the HRT $\beta_{\text{coex}} \simeq 0.345$ [12], the best theoretical estimate being $\beta_{\text{coex}} \simeq 0.327$ [24]. Moreover, in the SCOZA, as well as in the HRT, the critical point, identified as the top of the coexistence curve, coincides with that determined by locating the divergence of the isothermal compressibility as given by the compressibility sum rule. As a consequence, at the critical point one has both coalescence of the vapor and liquid phases and occurrence of long-range correlations, as expected. Because of the lack of thermodynamic consistency, this is not the case with LOGA/ORPA, in which the critical point obtained by the compressibility route corresponds to the top of the spinodal curve shown in Fig. 3.

We now consider the radial distribution function $g(r)$. The SCOZA $g(r)$ has been determined using both closure (2.1) and (2.17). In Fig. 5 the SCOZA and LOGA/ORPA results for two different states are compared with MC simulations. We see that, while the overall agreement is satisfactory, the behavior near contact is not reproduced very well. It is unlikely that this can be traced back to the slight inaccuracy in the treatment of the hard-sphere contribution to $c(r)$ for $r > 1$ entailed by Eq. (2.1) or (2.17). In fact, such a contribution is accurately taken into account in LOGA/ORPA, which nevertheless does not appear to perform better than SCOZA. In particular, using closure (2.17) in SCOZA produces results for $g(r)$ which are undistinguishable from those of LOGA/ORPA, at least for the states we investigated. Moreover, we checked that for the densities considered here the hard-sphere $g(r)$ obtained from closure (2.17) in the high-temperature limit is nearly superimposed to that given by the Waisman parameterisation. On the other hand, both in SCOZA and in

LOGA/ORPA the contribution to $c(r)$ due to the tail potential $w(r)$ is bound to follow the profile of $w(r)$ itself for all r 's. Such a form is best suited for interactions that are slowly varying on a lengthscale of the order of the particle size, while the two-Yukawa tail of Eq. (1.1) changes quite steeply near its minimum. As is well known, such a problem is usually dealt with by splitting the potential according to the WCA prescription [11], but implementing this procedure in the SCOZA seems very artificial, as it would hinder the analytical tractability of the system, which is the very reason why the HC2YF interaction (1.1) was considered in the first place instead of the LJ potential.

Since on the basis of the comparison with MC results the SCOZA proves to accurately reproduce the coexistence curve of the HC2YF, it could be worthwhile using it to assess the ability of different HC2YF parameterisations of the LJ potential to reproduce the LJ coexistence curve. To this end, in Fig. 6 we have compared the coexistence curve of the LJ potential given by MC simulations [25] with the SCOZA results using closure (2.17) for the parameterisations proposed by Sun [4,7] and by Foiles and Ashcroft [6], together with that of Eq. (1.1). We see that the HC2YF form of Eq. (1.1), closely resembling that of Ref. [9], gives the best representation of the LJ potential among those considered here, at least as far as the liquid-vapor phase diagram is concerned.

In summary, we have presented SCOZA results for the phase diagram and the correlations of a two-Yukawa parameterisation of the LJ potential. These have been compared with the predictions of other theories and with new MC simulation data. The comparison shows that the SCOZA provides a very accurate coexistence curve, with a critical point that differs from the prediction of MC supplemented by finite-size scaling techniques by less than 1%. At the same time, the two-Yukawa potential we studied, closely resembling that previously proposed by Kalyuzhnyi and Cummings [9], reproduces satisfactorily the LJ coexistence curve. In view of the very good performance of SCOZA in predicting the liquid-vapor phase diagram of simple fluids, we think that it could be worthwhile to generalize the solution procedure, so that it will not be confined anymore to tail potentials of Yukawa form. This could also allow one to implement SCOZA with a more sophisticated closure than the forms (2.1) and (2.17) used here.

ACKNOWLEDGMENTS

N.B.W. thanks the Royal Society (grant number 19076), the Royal Society of Edinburgh and the EPSRC (grant no. GR/L91412) for financial support. D.P. thanks the National Science Foundation for financial support while visiting Stony Brook. G.S. gratefully acknowledges the support of the Division of Chemical Sciences, Office of Basic Energy Sciences, Office of Energy Research, U.S. Department of Energy.

TABLES

	MC [†]	SCOZA [★]	SCOZA [●]	HRT	LOGA _{en} [‡]	LOGA _{comp} [◇]
ρ_c^*	0.310(1)	0.307	0.304	0.310	0.314	0.328
T_c^*	1.295(1)	1.304	1.293	1.316	1.352	1.071

TABLE I. Critical density and temperature (in reduced units) for the HC2YF. †: MC simulation performed in this work. ★: SCOZA result using 2-Yukawa $c(r)$ of Eq. (2.17). ●: SCOZA result using 2-Yukawa $c(r)$ of Eq. (2.1). ‡: LOGA/ORPA result using energy route. ◇: LOGA/ORPA result using compressibility route.

FIGURES

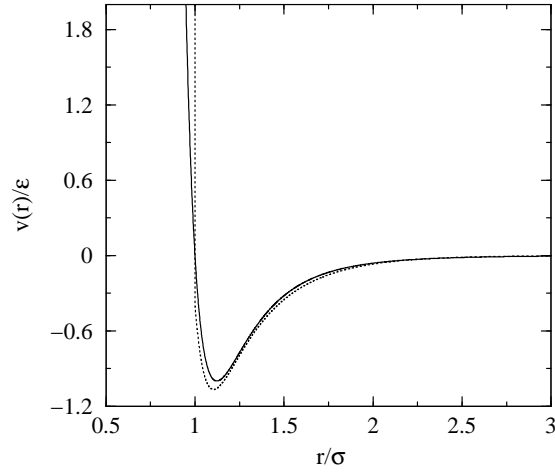


FIG. 1. Pair potentials of the interparticle interaction given by the LJ fluid (dotted curve) and the HC2YF (full curve) of Eq. (1.1) with amplitude and range parameters specified in the text.

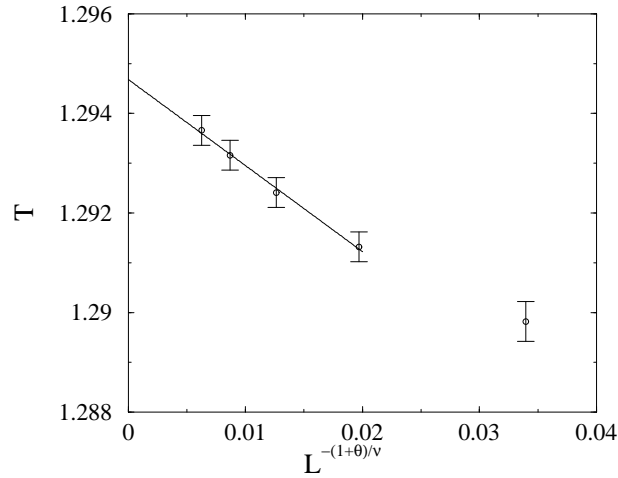


FIG. 2. The apparent reduced critical temperature (as defined by the matching condition described in the text and in [16]), plotted as a function of $L^{-(\theta+1)/\nu}$, with $\theta = 0.54$ and $\nu = 0.629$. The extrapolation of the least squares fit to infinite volume yields the estimate $T_c^* = 1.295(1)$.

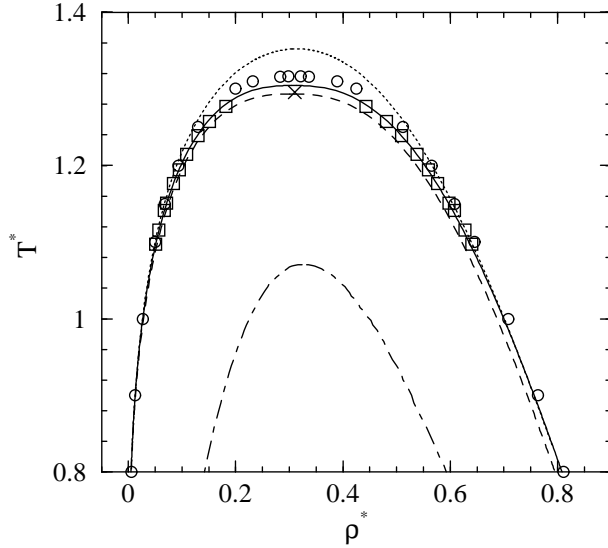


FIG. 3. Coexistence curve of the hard-core two-Yukawa fluid in the density-temperature plane. Density and temperature are in reduced units. Solid line: SCOZA with closure (2.17) and Carnahan-Starling reference system thermodynamics (see text). Dashed line: SCOZA with closure (2.1) and Percus-Yevick reference system thermodynamics. Dotted line: LOGA/ORPA (energy route). Circles: HRT. Squares: MC simulation performed in this work. Cross: MC critical point. Dot-dashed line: LOGA/ORPA spinodal curve (compressibility route).

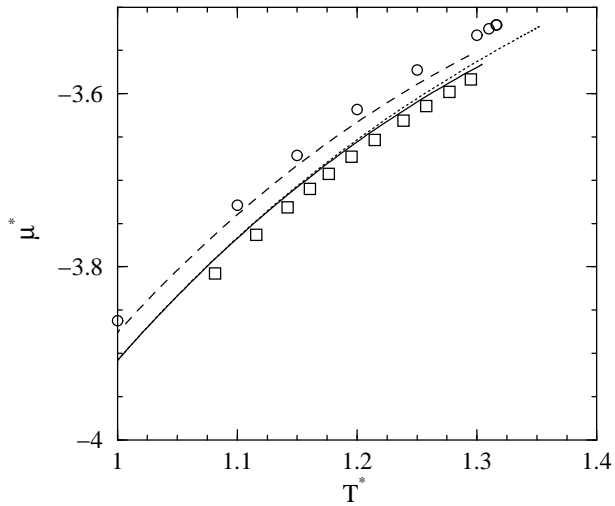


FIG. 4. Coexistence curve in the T^* - μ^* plane. Symbols as in Fig. 3

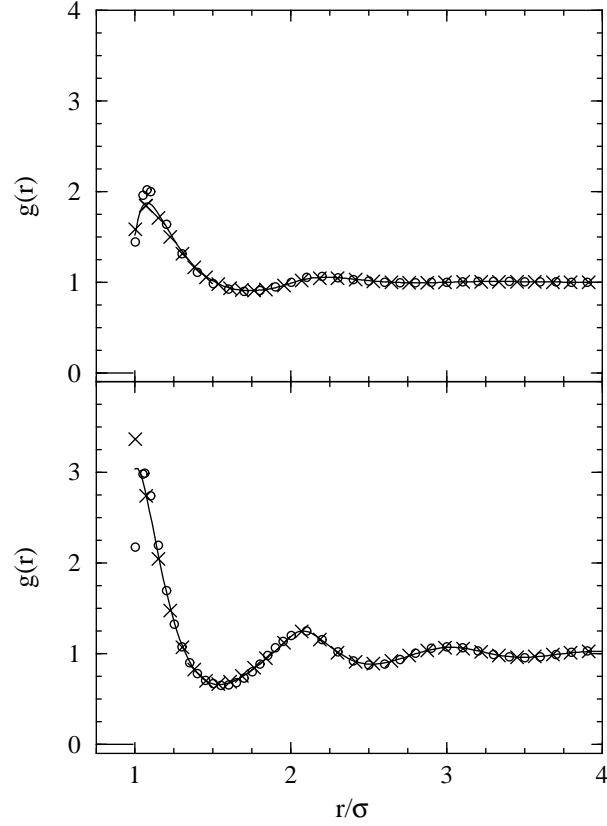


FIG. 5. Radial distribution function of the HC2YF at $T^* = 1.5$, $\rho^* = 0.4$ (upper panel) and $T^* = 1$, $\rho^* = 0.8$ (lower panel). Solid line: SCOZA with closure (2.1). Crosses: LOGA/ORPA. Circles: MC simulation. The result of SCOZA with closure (2.17) are undistinguishable from those of LOGA/ORPA.

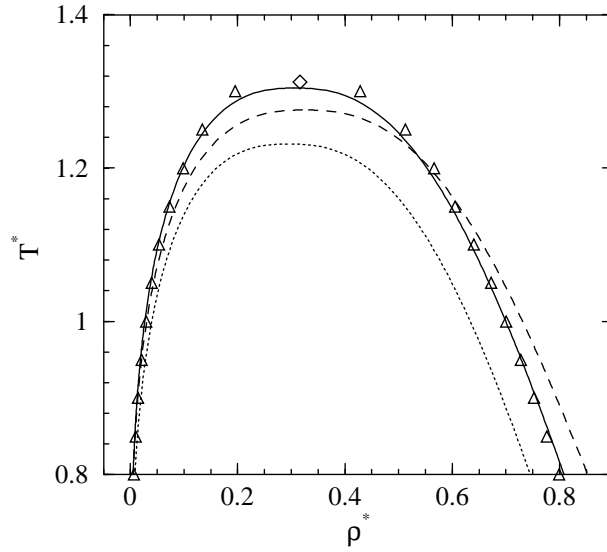


FIG. 6. Comparison between the LJ and the HC2YF coexistence curve for different HC2YF parameterisations. Lines: SCOZA results for the HC2YF of Eq. (1.1) with amplitude and range parameters by Kalyuzhnyi and Cummings (solid line), by Foiles and Ashcroft [6] (dotted line), and by Sun [4,7] (dashed line). Triangles: MC simulation results for the LJ coexistence curve [25]. Diamond: MC simulation result for the LJ critical point [26].

REFERENCES

- [1] Y. Rosenfeld, *J. Chem. Phys.* **98**, 8126 (1993).
- [2] C. Caccamo, G. Giunta and G. Malescio, *Mol. Phys.* **84**, 125 (1995).
- [3] D. Pini, G. Stell and N. B. Wilding, *Mol. Phys.* **95**, 483 (1998).
- [4] S. Sun, Ph.D. thesis, State University of New York at Stony Brook (1976).
- [5] C. Jedrzejek and G. A. Mansoori, *Acta Phys. Pol.* **A57**, 107 (1980).
- [6] S. M. Foiles and N. W. Ashcroft, *Phys. Rev.* **A24**, 424 (1981).
- [7] J. Konior and C. Jedrzejek, *Mol. Phys.* **63**, 655, (1988).
- [8] E. N. Rudisill and P. T. Cummings, *Mol. Phys.* **68**, 629 (1989).
- [9] Y. V. Kalyuzhnyi and P. T. Cummings, *Mol. Phys.* **87**, 1459 (1996).
- [10] J. A. Barker and D. Henderson, *J. Chem. Phys.* **47**, 4714 (1967).
- [11] J. D. Weeks, D. Chandler, and H. C. Andersen, *J. Chem. Phys.* **54**, 5237 (1971).
- [12] A. Parola and L. Reatto, *Adv. Phys.* **44** 211 (1995).
- [13] J. S. Høye, G. Stell, and E. Waisman, *Mol. Phys.* **32**, 209 (1976); J. S. Høye and G. Stell, *ibid.* **52**, 1057 (1984); J. S. Høye and G. Stell, *ibid.* **52**, 1071 (1984).
- [14] E. Waisman, *Mol. Phys.* **25**, 45 (1973).
- [15] D. Pini, G. Stell, and J. S. Høye, *Int. J. Thermophys.* **19**, 1029 (1998).
- [16] N. B. Wilding, *Phys. Rev. E* **52**, 602 (1995); N. B. Wilding and A. D. Bruce *J. Phys. Condens. Matter* **4**, 3087.(1992).
- [17] D. Frenkel and B. Smit, *Understanding Molecular Simulation*, Academic Press, Boston, (1996).
- [18] A. M. Ferrenberg and R. H. Swendsen, *Phys. Rev. Lett.* **61**, 2635 (1988); *ibid.* **63**, 1195 (1989).
- [19] B. Berg and T. Neuhaus, *Phys. Rev. Lett.* **68**, 9 (1992).
- [20] It should be noted that a different form of field mixing involving pressure terms in the relevant scaling fields has recently been proposed by M. E. Fisher and G. Orkoulas, *Phys. Rev. Lett.* **85**, 696 (2000); G. Orkoulas, M. E. Fisher, and C. Ustun, *J. Chem. Phys.* **113**, 7530 (2000). This modification has not been considered in the present work.
- [21] G. Stell, *J. Chem. Phys.* **55**, 1485 (1971).
- [22] H. C. Andersen and D. Chandler *J. Chem. Phys.* **57**, 1918 (1972).
- [23] J. S. Høye, D. Pini, and G. Stell, *Physica* **A279**, 213 (2000).
- [24] J. Zinn-Justin, *Quantum Field Theory and Critical Phenomena* (Clarendon, Oxford, 1983).
- [25] A. Lotfi, J. Vrabec, and J. Fischer, *Mol. Phys.* **76**, 1319 (1992).
- [26] J. J. Potoff and A. Z. Panagiotopoulos, *J. Chem. Phys.* **109**, 10914 (1998).